BULLETIN DE L'ASSOCIATION MINÉRALOGIQUE DU CANADA

THE CANADIAN MINERALOGIST

JOURNAL OF THE MINERALOGICAL ASSOCIATION OF CANADA

Volume 37 February 1999 Part 1

The Canadian Mineralogist
Vol. 37, pp. 1-15 (1999)

MEASURING MINERAL ABUNDANCE IN SKARN. I. THE RIETVELD METHOD USING X-RAY POWDER-DIFFRACTION DATA

MATI RAUDSEPP[1], ELISABETTA PANI AND GREGORY M. DIPPLE

Department of Earth and Ocean Sciences, The University of British Columbia, Vancouver, British Columbia V6T 1Z4

ABSTRACT

We evaluate the Rietveld method for determining mineral abundance in natural and synthetic wollastonite skarn using X-ray powder-diffraction data. The results have promise for petrological applications that require modal analysis of large, heterogeneous samples and for mineral-exploration programs. Our main objective was to develop a practical procedure for rapid quantitative modal analysis with the Rietveld method using a conventional Bragg–Brentano X-ray diffractometer. Simulated samples of wollastonite ore were prepared from single-mineral powders, and the experimentally determined modes were compared to the nominal modes. For samples containing 30–99 wt.% wollastonite, the relative error ranges from 0.04 to 1.3%. For phases other than wollastonite, the relative error is generally dependent on the amount present. Above concentrations of 6 wt.%, the relative error is 6%, decreasing at high concentrations to about 1%. Below concentrations of 6 wt.%, the relative error increases rapidly. In addition, twenty drill-core samples from the Isk deposit, in northwestern British Columbia, containing up to thirteen phases, were analyzed with the Rietveld method. The results were compared to mineral abundances determined with a whole-rock chemical analysis and projection method. Determinations of wollastonite abundance by the two methods are in excellent agreement, except for certain samples with mineral assemblages atypical of the Isk wollastonite skarns. The discrepancy between the two methods therefore most likely results from invalid assumptions in the projection method.

Keywords: Rietveld refinement, modal analysis, X-ray powder-diffraction, wollastonite, skarn, Isk deposit, British Columbia.

SOMMAIRE

Nous évaluons la méthode de Rietveld afin d'établir la proportion des minéraux, dont la wollastonite, dans des échantillons de skarn naturels et synthétiques en utilisant des données de diffraction X sur poudre. Les résultats sont promettants pour les applications pétrologiques exigeant des proportions modales de minéraux de gros échantillons hétérogènes et pour les programmes d'exploration minérale. Notre objectif principal était de développer une procédure pratique d'analyser quantitativement et rapidement la proportion modale de minéraux à partir de la méthode de Rietveld en utilisant un diffractomètre conventionnel à configuration Bragg–Brentano. Des échantillons simulés de minerai de wollastonite ont été préparés en mélangeant des poudres monominérales, et les proportions modales déterminées expérimentalement ont été comparées avec les proportions nominales. Dans le cas des échantillons contenant de 30 à 99% de wollastonite (base pondérale), l'erreur relative varie entre 0.04 et 1.3%. Pour les phases autres que la wollastonite, l'erreur relative est généralement dépendante de la proportion. Dans le cas des concentrations dépassant 6% (poids), l'erreur relative est 6%, diminuant aux concentrations élevées à moins de 1%. En-dessous d'un seuil de 6%, l'erreur relative augmente rapidement. En plus, vingt échantillons de carottes provenant du gisement de Isk, dans le nord-ouest de la Colombie-Britannique, contenant jusqu'à treize phases, ont été traitées de la même façon. Les résultats sont

[1] *E-mail address*: mraudsepp@eos.ubc.ca

comparés aux abondances de minéraux déterminées selon la composition chimique globale et une méthode de projection. Les résultats des deux méthodes d'évaluer la teneur en wollastonite concordent étroitement sauf dans le cas de certains échantillons contenant des assemblages atypiques pour les skarns de ce gisement. Le décalage entre les deux méthodes proviendrait de suppositions non valides dans la méthode des projections.

(Traduit par la Rédaction)

Mots-clés: affinement de Rietveld, analyse modale, diffraction X, méthode des poudres, wollastonite, skarn, gisement de Isk, Colombie-Britannique.

Introduction

Knowledge of the relative abundances of the constituent minerals in a sample of rock is not only important for purposes of classification and to determine paragenesis, but is also essential to the characterization, economic extraction and concentration of potentially valuable ores. Traditionally, modal analysis has been done in one of three ways: (1) point-counting of thin sections or slabs of rock using an optical microscope, scanning electron microscope or electron microprobe (visual methods), (2) conventional X-ray powder-diffraction measurements using integrated peak-intensities and some scheme of external or internal calibration, and (3) mass-balance calculations that convert a whole-rock chemical composition into mineral abundances.

We have been developing techniques for the rapid, inexpensive and accurate determination of wollastonite content in skarn from the Isk deposit in northwestern British Columbia. Delineation of wollastonite zones of high purity is essential to assess the economic potential of the deposit. The exploration program produced large, heterogeneous samples of skarn (two-m intervals of diamond drill-core and bulk trench-samples), which required bulk crushing and thorough mixing prior to analysis. Visual estimates have proven unreliable for these disaggregated samples because of the acicular nature of wollastonite and the preferential settling of mineral grains other than wollastonite during the preparation of sample mounts from powder. We have therefore focused on X-ray powder-diffraction and whole-rock chemical techniques. In this paper, we describe and evaluate two methods of determining mineral abundance in wollastonite skarn: a Rietveld method that uses X-ray powder-diffraction data and a projection method that uses whole-rock chemical data. In a companion paper, Gordon & Dipple (1999) describe a linear programming formulation that uses whole-rock chemical data and compare results of all three methods.

Choice of X-Ray Powder-Diffraction Technique for Modal Analysis

Conventional X-ray powder-diffraction measurements of the integrated intensities of peaks using calibration curves and internal standards are troublesome because of the difficulty of obtaining and preparing standards with degrees of crystallinity, composition and micro-absorption similar to those of the unknowns. In addition, the X-ray-diffraction patterns of rocks (*e.g.*, various types of skarns) can be extraordinarily complex, with hundreds or even thousands of overlapping peaks which make it difficult, if not impossible, to find any peaks suitable for measuring integrated intensities. A very comprehensive review of the relative merits of each of the above methods is given by Hill *et al.* (1993).

For the purpose of this study, to overcome most of the problems associated with traditional X-ray methods, we used the Rietveld method, a full-profile approach to quantitative phase-analysis. The Rietveld method generates a calculated diffraction-pattern that is compared with the observed data; the structural parameters of each mineral (atomic coordinates, site occupancies, displacement parameters), together with various experimental parameters affecting the pattern, are refined by least-squares procedures to minimize the difference between the complete observed and calculated diffraction-patterns. From the refined site-occupancies at each atomic position in the structure, accurate element-order parameters at each site *and* (in principle) the bulk composition of the material can be derived. Originally developed for the refinement of relatively simple structures investigated with neutron-diffraction data (Rietveld 1967, 1969), the method was subsequently applied with X-ray-diffraction data to crystal-structure refinements of simple to complex rock-forming minerals and synthetic equivalents (*e.g.*, Young *et al.* 1977, Hill 1984, Baerlocher & Schicker 1987, Raudsepp *et al.* 1990, Bish 1993). A detailed summary of crystal-structure applications of the Rietveld method is given by Post & Bish (1989).

Of particular relevance to doing modal analysis of rocks is the fact that the Rietveld refinement method can be used to characterize more than one phase simultaneously, and more significantly, that the relative masses of all phases contributing to the diffraction pattern can be derived from the refinement using the relationship (Hill & Howard 1987):

$$W_r = S_r (ZMV)_r / \sum_t S_t (ZMV)_t$$

where W_r is the *relative* weight fraction of phase r in a mixture of t phases, S is the scale factor derived from Rietveld refinement, Z is the number of formula units

per unit cell, M is the mass of the formula unit (atomic mass units), and V is the volume of the unit cell (Å^3). This relationship holds if all of the phases are well crystallized and free of preferred orientation, and have similar degrees of micro-absorption of X-rays. Excellent reviews and applications of the Rietveld method as a technique for modal analysis have been published during the past 10 years (*e.g.,* Hill & Howard 1987, Bish & Howard 1988, Hill 1991, Bish & Post 1993, Hill *et al.* 1993, Mumme *et al.* 1996a, b).

All natural samples used in this study derive from the Bril locality, one of five zones of wollastonite skarn located in the Iskut River map-area of northwestern British Columbia, immediately east of the boundary between the Coast and Intermontane belts. The skarns are collectively known as the Isk deposit and are located exclusively within limestone of the Stikine assemblage, where it is in direct contact with the Zippa Mountain syenite (Jaworski & Dipple 1996). The study was done in three parts:

1. A sample of >99% pure Bril wollastonite concentrate was refined with the Rietveld method to check for impurities, to assess the effects of potentially extreme preferred orientation of a major phase with markedly anisotropic shape of grains, and to determine if more than one polytype is present.

2. Nine carefully prepared samples of simulated wollastonite ore were analyzed; the experimentally determined modes were compared to the nominal modes to test the validity of doing a modal analysis on these samples with the Rietveld method.

3. Twenty natural drill-core samples from the Bril locality were analyzed, and the results from the Rietveld refinements were compared to modal analyses derived from whole-rock chemical compositions.

This paper highlights our success in determining mineral abundance in natural and synthetic skarn using the Rietveld method with X-ray powder-diffraction data. Our results have promise for petrological applications that require modal analysis of large, heterogeneous samples and for exploration programs.

Experimental Methods

Sample preparation

Simulated typical wollastonite ores spanning a range of compositions were prepared by weighing out various proportions of five components: wollastonite, quartz, calcite, microcline, and almandine (Table 1). Quartz, calcite and microcline were acquired from the M.Y. Williams Geological Museum (The University of British Columbia), wollastonite from the Bril wollastonite concentrate, Zippa Mountain, British Columbia, and almandine from Gore Mountain, New York. All of the components except microcline were >99% single-phase. The microcline is perthitic and contains 5% albite; the wollastonite contains trace amounts of quartz, albite, and microcline. Chemical compositions of each phase were determined either by electron-probe micro-analysis or by energy-dispersion X-ray spectrometry (EDS) (Table 1). The nominal amount of microcline weighed was corrected to account for the amount of exsolved albite (Table 1).

The particle size of each phase was reduced to less than 0.5 mm in diameter using a steel ring mill. Final grinding to the optimum grain-size range for X-ray analysis (<10 μm) was done under ethanol in a vibratory McCrone Micronising Mill (McCrone Scientific Ltd., London, U.K.) for 20–30 minutes. Fine grain-size is an important factor in reducing micro-absorption contrast between phases (Brindley 1945). After weighing, the mixtures were further ground for about 10 minutes to ensure complete mixing. Sample preparation for the natural samples from the Bril drill core was similar to that of the simulated samples except that the Bril samples had been previously ground to <200 mesh for chemical analysis. Prior to collecting the X-ray-diffrac-

TABLE 1. NOMINAL MODAL COMPOSITION OF SIMULATED WOLLASTONITE ORES (WT.%)

	1	2	3	4	5	6	7	8	9
Wollastonite[1]	79.79	49.98	69.88	89.94	98.84	30.45	30.10	29.99	30.10
Quartz[2]	8.00	15.99	7.03	1.03	0.13	15.01	4.00	4.73	40.00
Calcite[3]	5.13	12.03	8.00	4.96	0.30	6.96	19.95	30.16	0.00
Almandine[4]	3.98	4.03	3.03	2.03	0.40	7.98	42.96	5.03	3.47
Microcline[5]	2.95	17.06	11.46	1.93	0.32	37.61	2.85	28.59	25.11
Albite[6,7]	0.16	0.90	0.60	0.10	0.02	1.98	0.15	1.50	1.32
	100.00	100.00	100.00	100.00	100.00	100.00	100.00	100.00	100.00

Notes

[1] $Ca_{1.98}Fe_{0.02}Si_{2.00}O_3$ (electron-probe micro-analysis, no. of cations on the basis of 3 O)

[2] Pure quartz from clear, colorless crystal

[3] Pure calcite (energy-dispersion X-ray analysis shows trace Fe, Mn, Mg)

[4] $(Ca_{0.32}Fe_{1.56}Mn_{0.04}Mg_{1.03})Al_{2.04}Ti_{0.01}Si_{2.96}O_{12}$ (XRF analysis, no. of cations on the basis of 12 O)

[5] $K_{0.94}Na_{0.04}Al_{1.02}Si_{2.99}O_8$ (electron-probe micro-analysis, no. of cations on the basis of 8 O)

[6] $Na_{0.99}Al_{1.00}Si_{3.00}O_8$ (electron-probe micro-analysis, no. of cations on the basis of 8 O)

[7] Mode determined by image analysis of perthite in thin section

tion data, these powders were further ground in the McCrone Micronising Mill for 20 minutes. A consequence of grinding both the simulated and natural samples was the addition of corundum abraded from the grinding elements; corundum contamination was treated as an additional phase in the Rietveld refinements.

Samples of the Bril wollastonite concentrate (Fig. 1A) and each simulated ore (*e.g.*, Fig. 1B) were examined for grain size and shape using a scanning electron microscope (SEM). In general, the grain size after grinding varied from less than 1 μm to 20–30 μm, averaging about 5 μm. Because of their acicular habit, a few crystals of wollastonite measured up to about 50–100 μm in length. The Bril drill core samples were examined also in the unground state using SEM–EDS to check for grain size, shape and the presence of minerals in amounts too small to be refined. Trace amounts of hydroxylapatite, pyrite, zircon, barite and magnetite were found to be present.

Collection of X-ray powder-diffraction data

Samples were first pressed from the bottom of an aluminum sample holder against a ground glass slide; the cavity in the holder measures 43 × 24 × 1.5 mm. The textured surface of the glass minimizes preferred orientation of anisotropic grains in the part of the powder that is pressed against the glass. Before collecting X-ray-diffraction data from the other samples, the pure wollastonite concentrate was analyzed in detail to assess the degree of preferred orientation and to check for extraneous phases. Trial data-collections and refinements showed that the above mounting procedure was inadequate to overcome the severe preferred orientation of wollastonite grains, and subsequent samples were serrated with a razor blade in two directions, perpendicular and parallel to the axis of the goniometer. This treatment of the surface gave the least preferred orientation, and all other samples (simulated and natural) were subsequently prepared with two directions of serrations. The disadvantages of serrating the surface of the sample include a slight loss of overall diffraction-intensity, broader peaks and degradation of displacement parameters because of surface roughness; however, these effects are insignificant compared to the large errors introduced by preferred orientation.

Step-scan X-ray powder-diffraction data were collected over a range 8–70°2θ with Cu$K\alpha$ radiation on a standard Siemens D5000 Bragg–Brentano diffractometer equipped with a diffracted-beam graphite monochromator crystal, 2 mm (1°) divergence and antiscatter slits, 0.6 mm receiving slit and incident-beam Soller slit. The long sample holder used (43 mm) ensured that the area irradiated by the X-ray beam under these conditions was completely contained within the sample. The diffracted-beam Soller slit was removed, as the intensity of the diffraction pattern was increased three times, and no major phase has peaks at very low angles of diffraction. The long fine-focus Cu X-ray tube was operated at 40 kV and 30 mA, using a take-off angle of 6°. Although various step-sizes and counting times were used for special refinements (Tables 2, 3 and see below), the best compromise between acceptable precision and rapid collection of the data was a step size of 0.04°2θ and a counting time of 2 s/step. Details of data collection and Rietveld refinements are given in Tables 2 and 3.

Rietveld refinement and modal analysis

X-ray powder-diffraction data were refined with the Rietveld program DBWS–9411 (Young *et al.* 1994,

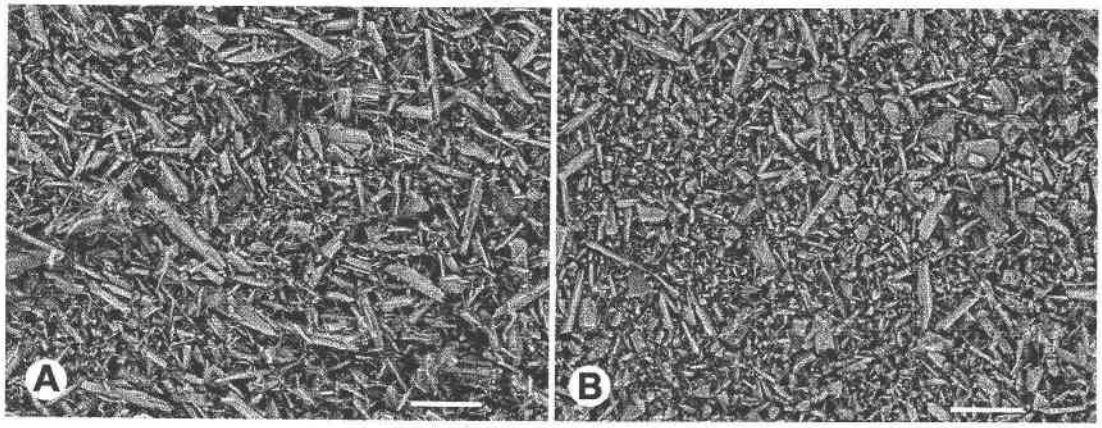

FIG. 1. A. Back-scattered electron micrograph of Bril wollastonite concentrate after grinding. B. Back-cattered electron micrograph of typical sample of simulated wollastonite ore after grinding. Scale bar is 20 μm in both cases.

TABLE 2. DETAILS OF DATA COLLECTION AND RIETVELD REFINEMENT OF BRIL WOLLASTONITE AND SIMULATED ORES

	Bril	1A	1B	2	3	4	5	6	7	8	9
scanning range (°2θ)	8-70	8-70	8-70	8-70	8-70	8-70	8-70	8-70	8-70	8-70	8-70
step (°2θ)	0.02	0.04	0.08	0.04	0.04	0.04	0.04	0.04	0.04	0.04	0.04
counting time/step (s)	20	2	2	2	2	2	2	2	2	2	2
scanning time (minutes)	1033	52	26	52	52	52	52	52	52	52	52
[1]no. of phases	4	7	7	8	8	7	7	8	7	8	7
R_p	7.8	10.0	14.7	8.8	10.4	10.0	12.2	8.9	10.7	9.5	8.0
R_{wp}	10.2	13.2	19.9	11.8	14.3	13.4	16.1	11.7	14.2	12.5	11.0
R_{exp}	5.8	9.8	17.2	9.2	9.5	9.7	9.8	8.9	10.4	9.7	8.5
S (Goodness of fit)	1.8	1.3	1.1	1.3	1.5	1.4	1.6	1.3	1.4	1.3	1.3

[1] includes corundum (contamination from grinding)

TABLE 3. DETAILS OF DATA COLLECTION AND RIETVELD REFINEMENT OF BRIL DRILL-CORE SAMPLES

	3810	5270	2760	420	2610	4820	1270	3395	5795	3470	2595	6360	3600	5000	4400	360	5195	2795	4995	2995
[1]no. of phases	12	12	12	12	12	12	12	12	12	12	12	12	12	13	12	12	12	14	12	14
R_p	9.3	9.8	9.4	9.1	9.2	8.6	12.5	9.5	9.3	8.4	9.2	9.6	9.0	8.4	9.8	9.4	9.4	10.4	10.2	10.2
R_{wp}	12.5	13.1	12.4	12.1	12.4	11.6	16.1	12.7	12.2	11.1	12.3	12.6	11.8	11.1	12.7	12.6	12.4	13.7	13.6	13.6
R_{exp}	9.6	9.8	9.8	9.8	9.9	9.8	9.8	10.1	10.0	9.7	10.5	9.8	10.1	8.6	9.1	10.2	9.9	9.8	10.3	9.9
S (Goodness of Fit)	1.3	1.3	1.3	1.2	1.2	1.2	1.6	1.2	1.2	1.1	1.2	1.3	1.2	1.3	1.4	1.2	1.2	1.4	1.3	1.4

2θ scan range, 8-59°; step interval, 0.04°2θ; integration time/step, 2 s; collection time, 43 min.
[1]includes corundum (contamination from grinding).

Young 1995) running on a Pentium Pro 200 MHz personal computer. Refinement times ranged from about 15 s/cycle (8 phases) to 45 s/cycle (14 phases). In general, the following refinement procedure was used, but it was slightly modified depending on the particular composition of a sample. Peaks were defined as being pseudo-Voigt with a variable percentage of Gaussian–Lorentzian character. The peak full-width at half-maximum (FWHM) was varied as a function of 2θ using the expression $H_k^2 = U\tan^2\theta + V\tan\theta + W$ of Caglioti *et al.* (1958) for major phases, but only W was refined for minor phases. The profile step-intensity was calculated over an interval of 4–6 FWHM on either side of each peak centroid, and peak asymmetry was corrected using the relation of Rietveld (1969). The background was refined with a polynomial function. A correction for preferred orientation (March–Dollase model) was refined only for major phases of anisotropic habit (*e.g.*, wollastonite, feldspar, pyroxene). Starting values for the atomic positions and cell dimensions for each phase were obtained from published crystal-structure refinements of minerals with compositions similar to those in the samples (Table 4). Isotropic displacement parameters of individual atoms were fixed at values extracted from single-crystal refinements of the structures.

The full 2θ-range (8–70°) was used for 8-phase refinements of the simulated ores. As the number of peaks in the diffraction pattern increases dramatically at high angles of diffraction, the 2θ-range for the natural samples was reduced to 8–59°. For example, a typical 12-phase diffraction pattern of wollastonite ore contains 3,460 $K\alpha_1 + K\alpha_2$ peaks in the range 8–70°2θ; in the range 8–59°2θ, the number of peaks is reduced to 2,200. This decrease in 2θ-range did not significantly change the results, and had the additional benefit of reducing the time required for collection of the X-ray data.

Refinements for quantitative phase-analysis were done in the following general sequence: surface displacement and zero-order background parameter, scale factors for all major phases, the second- and third-order background parameters, W peak parameters for the major phases, cell dimensions of the major phases, asymmetry parameters for the major phases, pseudo-Voigt

TABLE 4. SOURCES OF CRYSTAL-STRUCTURE DATA AND STARTING COMPOSITIONS OF MINERALS USED IN RIETVELD REFINEMENTS

Mineral	Crystal Structure	Starting Composition
Albite	Ambruster *et al.* (1990)	$NaAlSi_3O_8$
Almandine	Ambruster *et al.* (1992)	$Fe_3Al_2Si_3O_{12}$
Andradite	Lager *et al.* (1989)	$Ca_3Fe_2Si_3O_{12}$
Apatite	Hughes *et al.* (1989)	$Ca_5(PO_4)_3(OH)$
Phlogopite	Brigatti & Davoli (1990)	$K(Mg,Fe)_3(Al,Fe)Si_3O_{10}(OH,F)_2$
Calcite	Effenberger *et al.* (1981)	$CaCO_3$
Corundum	Lewis *et al.* (1982)	Al_2O_3
Diopside	Levien & Prewitt (1981)	$CaMgSi_2O_6$
Grossular	Hazen & Finger (1978)	$Ca_3Al_2Si_3O_{12}$
Microcline	Dal Negro *et al.* (1978)	$KAlSi_3O_8$
Pargasite	Makino & Tomita (1989)	$Na_{0.95}Ca_{1.99}Mg_{4.1}Fe_{0.9}(Al_{2.04}Si_{5.96})O_{22}(OH)_2$
Plagioclase	Phillips *et al.* (1971)	$Na_{0.99}Al_{1.00}Si_{3.00}O_8$
Quartz	Le Page & Donnay (1976)	SiO_2
Titanite	Hawthorne *et al.* (1991)	$CaTiO_5$
Wollastonite-1*A*	Ohashi (1984)	$CaSiO_3$
Wollastonite-2*M*	Ohashi (1984)	$CaSiO_3$

mixing parameter for the major phases, and preferred orientation parameters for major phases with marked grain-shape anisotropy. At this stage, the same parameters were successively refined for each minor phase to the point where the least-squares procedure reached a minimum or became unstable; phases that could not be successfully refined (generally those present in amounts less than 1%) were deleted from the refinement.

The progress of the refinement was monitored closely by examining the contribution of each phase to the pattern on the difference plot. Phases in concentrations greater than about 30–50% were also refined further. For example, depending on the composition of the sample, the remaining parameters in the Caglioti expression, asymmetry parameters, pseudo-Voigt mixing parameters, site occupancies, and overall displacement parameters were refined if the refinement remained stable, and if the fit of the calculated to observed patterns improved significantly. Site occupancies were refined only for the major phases; the compositions of minor phases were fixed at the literature values. In the case of the simulated wollastonite ores, the compositions of all phases were previously known, and the site occupancies were fixed at the nominal values. For the natural samples, wollastonite, quartz, calcite and corundum were assumed to be close to their nominal compositions, but the outcome of the refinements was much improved by refining the site occupancies of the major phases with variable cations. The quality of the fit between the calculated and observed diffraction-profiles was evaluated using standard indices of agreement, the profile *R*-factor R_p, the weighted profile *R*-factor R_{wp}, the expected *R*-factor R_{exp} and the goodness-of-fit index *S*, as defined in Young *et al.* (1994). As the multiphase diffraction profiles in these samples were severely overlapped and as many of the constituent phases were present in very low concentrations, we did not use the R_B index as a numerical criterion of fit. Results of the Rietveld refinements are given in Tables 5 and 6.

Modal analysis using a projection method and whole-rock chemical data

Mineral abundance in drill-core samples from the Bril skarn was independently determined from whole-rock chemical data. The major-element compositions of the samples were determined by X-ray fluorescence spectroscopy at the Cominco Exploration Laboratory in Vancouver, B.C. The weight fractions of whole-rock oxides were converted to mineral abundance through a change of basis that invoked additive and exchange components (Thompson 1982) on a molar basis. Additive components were chosen to be end-member compositions of minerals observed in the wollastonite skarn, and exchange components were chosen to allow for observed variation in mineral composition (Raudsepp, unpublished electron-probe data). The basis-transformation does not yield a unique solution for each sample because the new basis-set contains one more component than the initial basis-set. The transformation was therefore completed in two steps. The first transformation projects from titanite, hydroxylapatite, feldspar and calcite:

$$\begin{bmatrix} \text{Si} \\ \text{Al} \\ \text{Mg} \\ \text{Na} \\ \text{Mn} \\ \text{Fe} \\ \text{Ti} \\ \text{P} \\ \text{Ca} \\ \text{K} \\ \text{L.O.I.} \end{bmatrix} = \begin{bmatrix} 1 & 0 & 0 & 0 & 0 & 0 & 1 & 0 & 0 & 3 & 0 \\ 0 & 1 & 0 & 0 & 0 & 0 & 0 & 0 & 0 & 1 & 0 \\ 0 & 0 & 1 & 0 & 0 & 0 & 0 & 0 & 0 & 0 & 0 \\ 0 & 0 & 0 & 1 & 0 & 0 & 0 & 0 & 0 & 0 & 0 \\ 0 & 0 & 0 & 0 & 1 & 0 & 0 & 0 & 0 & 0 & 0 \\ 0 & -1 & -1 & 0 & -1 & 1 & 0 & 0 & 0 & 0 & 0 \\ 0 & 0 & 0 & 0 & 0 & 0 & 1 & 0 & 0 & 0 & 0 \\ 0 & 0 & 0 & 0 & 0 & 0 & 0 & 3 & 0 & 0 & 0 \\ 0 & 0 & 0 & 0 & 0 & 0 & 0 & 5 & 1 & 0 & 1 \\ 0 & 0 & 0 & -1 & 0 & 0 & 0 & 0 & 0 & 1 & 0 \\ 0 & 0 & 0 & 0 & 0 & 0 & 0 & 0.409 & 0 & 0 & 1 \end{bmatrix} \cdot \begin{bmatrix} \text{Si'} \\ \text{AlFe}_{-1} \\ \text{MgFe}_{-1} \\ \text{NaK}_{-1} \\ \text{MnFe}_{-1} \\ \text{Fe'} \\ \text{CaTiSiO}_5 \\ \text{Ca}_5\text{P}_3\text{O}_{12}(\text{OH}) \\ \text{Ca'} \\ \text{KAlSi}_3\text{O}_8 \\ \text{CaCO}_3 \end{bmatrix}$$

where loss on ignition (L.O.I.) is equated to whole-rock H_2O and CO_2 contained in hydroxylapatite and calcite, respectively. In the projection, the abundance of titanite, hydroxylapatite, feldspar and calcite is uniquely deter-

TABLE 5. [1]RESULTS OF RIETVELD REFINEMENT OF BRIL WOLLASTONITE AND SIMULATED ORES

	Bril	1A	1B	2	3	4	5	6	7	8	9
Wollastonite (wt.%)	99.14	79.23	78.98	49.96	69.09	88.73	98.06	30.48	29.68	30.16	29.77
[2]Relative error (%)	0.03	0.71	1.0	0.04	1.2	1.3	0.74	0.08	1.09	0.52	1.1
Quartz	0.86	7.93	7.98	17.13	7.14	1.33	0.99	15.19	4.97	4.78	40.77
Relative error (%)	1.1	0.82	0.25	7.1	1.9	33	893	1.3	24	1.6	1.9
Calcite	—	4.08	3.80	11.33	8.25	3.71	[3]n.r.	7.40	19.66	31.09	0.00
Relative error (%)	—	20	26	5.8	3.1	26	—	5.7	1.4	2.9	0
Almandine	—	4.11	4.66	3.91	3.44	2.21	0.67	7.98	43.01	4.65	3.37
Relative error (%)	—	3.2	17	2.9	14	10	68	0.28	0.12	7.1	2.6
Microcline	—	4.65	4.59	15.25	9.87	4.03	0.27	34.17	2.69	26.23	23.18
Albite	—	n.r.	n.r.	2.43	2.22	n.r.	n.r.	4.80	n.r.	3.10	2.90
Feldspar (total)	—	4.65	4.59	17.68	12.10	4.03	0.27	38.97	2.69	29.33	26.08
Relative error (%)	—	50	56	1.6	0.25	98	21	1.6	10	2.5	1.3

[1]Renormalized, corundum-free
[2]Relative error: Bril = e.s.d. from refinement
others = [(nominal abundance – abundance determined by Rietveld refinement)/nominal abundance] × 100.
[3]n.r. not refined

TABLE 6. [1]RESULTS OF RIETVELD REFINEMENT OF BRIL DRILL-CORE SAMPLES

WT.%	3810	5270	2760	420	2610	4820	1270	3395	5795	3470	2595	6360	3600	5000	4400	360	5195	2795	4995	2995
Wollastonite	90.4	81.9	81.1	76.5	75.1	70.1	65.5	58.2	55.1	54.5	43.4	36.7	31.6	27.5	26.4	23.9	0.76	0.39	0.37	0.36
Calcite	0.45	1.66	0.45	1.59	1.75	2.18	0.72	3.16	2.06	3.01	0.62	30.1	6.03	4.84	2.25	1.45	14.8	0.12	0.03	0.07
Grossular	0.06	3.89	5.17	9.44	10.1	2.63	17.7	0.02	0.88	3.70	10.3	6.21	11.5	4.44	5.30	6.37	0.42	0.01	0.35	0.43
Andradite	1.24	3.57	2.03	0.97	0.77	7.73	4.47	16.5	8.24	12.6	10.8	4.93	20.7	4.38	5.69	19.6	11.5	0.40	12.5	0.52
Diopside	5.96	6.18	5.97	7.65	9.22	13.5	9.36	13.0	30.2	7.54	31.4	17.0	16.4	3.20	17.2	40.5	61.4	83.1	80.8	77.0
Titanite	0.00	0.15	0.01	0.04	0.03	0.56	0.49	5.50	0.15	0.93	1.25	0.21	1.34	0.50	2.43	2.13	1.72	1.46	0.9	2.15
Quartz	0.80	0.45	1.06	0.54	0.92	1.16	0.74	1.40	1.10	1.44	0.47	1.02	3.38	2.13	1.64	1.01	6.96	0.93	0.79	0.84
Microcline	0.59	2.16	2.63	2.47	1.88	1.59	0.92	0.59	1.87	14.4	0.94	3.27	6.92	28.2	26.4	2.61	0.75	1.82	2.60	2.81
Apatite	0.53	0.03	0.75	0.67	0.10	0.47	0.16	1.50	0.37	0.67	0.80	0.51	0.62	0.36	0.13	1.94	1.18	5.11	1.64	5.20
Plagioclase	0.00	0.00	0.85	0.07	0.07	0.01	0.00	0.09	0.00	1.24	0.08	0.01	1.48	21.6	12.4	0.47	0.58	1.50	0.00	1.91
Pargasite	0.00	0.00	0.00	0.00	0.00	0.00	0.00	0.00	0.00	0.00	0.00	0.00	0.00	0.00	0.00	0.00	0.00	3.80	0.00	7.66
Biotite	0.00	0.00	0.00	0.00	0.00	0.00	0.00	0.00	0.00	0.00	0.00	0.00	0.00	2.92	0.00	0.00	0.00	1.31	0.00	1.07

MOLE %	3810	5270	2760	420	2610	4820	1270	3395	5795	3470	2595	6360	3600	5000	4400	360	5195	2795	4995	2995
Wollastonite	93.7	90.2	89.8	87.7	86.0	81.8	79.0	73.4	69.9	71.8	63.5	42.2	47.8	43.4	42.6	41.0	1.10	0.78	0.76	0.76
Calcite	0.54	2.13	0.58	2.11	2.32	2.96	2.41	4.62	3.03	4.61	1.06	40.2	10.6	8.87	4.22	2.88	24.9	0.29	0.06	0.17
Grossular	0.02	1.11	1.49	2.65	2.81	0.75	7.10	0.01	0.24	1.18	3.87	1.75	4.36	1.82	2.21	2.84	0.16	0.00	0.19	0.23
Andradite	0.31	0.90	0.54	0.26	0.21	2.10	0.23	4.94	2.50	4.01	3.61	1.33	7.44	1.65	2.18	8.00	3.96	0.19	6.10	0.26
Diopside	3.41	3.65	3.57	4.71	5.67	8.50	7.49	8.71	20.4	5.20	24.7	10.5	13.2	2.71	14.9	36.8	47.6	86.5	85.7	83.1
Titanite	0.00	0.10	0.01	0.03	0.02	0.39	0.46	4.11	0.12	0.74	1.08	0.15	1.20	0.46	2.31	2.16	1.48	1.73	1.08	2.65
Quartz	1.60	0.96	2.26	1.19	2.02	2.61	2.50	3.40	2.69	3.66	1.31	2.26	9.90	6.49	5.13	3.36	19.6	3.59	3.13	3.39
Microcline	0.26	0.99	1.21	1.18	0.89	0.78	0.70	0.32	0.99	7.93	0.57	1.56	4.36	18.6	17.8	1.86	0.45	1.52	2.22	2.45
Apatite	0.13	0.01	0.19	0.18	0.03	0.13	0.05	0.44	0.11	0.20	0.28	0.14	0.21	0.13	0.05	0.78	0.40	2.38	0.78	2.51
Plagioclase	0.00	0.00	0.40	0.03	0.04	0.00	0.00	0.05	0.00	0.70	0.05	0.00	0.97	14.8	8.69	0.35	0.37	1.31	0.00	1.72
Pargasite	0.00	0.00	0.00	0.00	0.00	0.00	0.00	0.00	0.00	0.00	0.00	0.00	0.00	0.00	0.00	0.00	0.00	1.03	0.00	2.15
Biotite	0.00	0.00	0.00	0.00	0.00	0.00	0.00	0.00	0.00	0.00	0.00	0.00	0.00	1.19	0.00	0.00	0.00	0.69	0.00	0.58

[1]Renormalized, corundum-free

mined. A second transformation produced minimum and maximum estimates of quartz, pyroxene, garnet and wollastonite content from the abundance of Si', Fe' and Ca' of the first transformation:

$$Si' \rightarrow CaSiO_3 \text{ or } SiO_2$$
$$Fe' \rightarrow CaFeSi_2O_6 \text{ or } Ca_3Fe_2Si_3O_{12}$$
$$Ca' \rightarrow CaSiO_3 \text{ or } Ca_3Fe_2Si_3O_{12}$$

The range of solutions corresponds to maximum forward and reverse progress within each sample of the reaction relationship:

$$CaSiO_3 + 2\ CaFeSi_2O_6 + 1/2\ O_2 = Ca_3Fe_2Si_3O_{12} + 2\ SiO_2$$

Results and Discussion

Simulated wollastonite ores

Before analyzing the simulated wollastonite ores, a highly precise set of data collected from the pure concentrate (Bril, Table 2) was refined in order to determine if more than one polytype of wollastonite is present and if the traces of quartz, microcline and albite observed by SEM could be detected. Two polytypes of wollastonite were detected, wollastonite-1*A* and wollastonite-2*M*. Microcline and albite were not detected in the first round of refinement, and subsequent refinements of the concentrate were done on the basis of four phases: wollastonite-1*A*, wollastonite-2*M*, quartz and corundum (contamination from grinding). The results of the refinement (Table 5, Fig. 2) showed that the concentrate is essentially pure wollastonite (99.14 wt.%) with a trace of quartz (0.86 wt.%). About 0.1 wt.% corundum was found to be present as contamination from grinding. The presence of wollastonite-2*M* was confirmed both by comparing the fit of the calculated X-ray patterns of wollastonite-1*A* and wollastonite-2*M* to the experimental pattern, and also by the presence of the $2\bar{1}1$ peak with *d*-value of 4.37 Å (Heller & Taylor 1956).

At first, our attempts to refine wollastonite-1*A* and wollastonite-2*M* independently gave poor results; although a fairly good fit of the calculated to the observed patterns was obtained, many of the minor peaks of both wollastonite polytypes were poorly fitted, the amount of wollastonite-2*M* was overestimated, and the total proportion of wollastonite was underestimated (Fig. 3A). These discrepancies stem from the fact that all of the major peaks of wollastonite-1*A* and wollastonite-2*M*

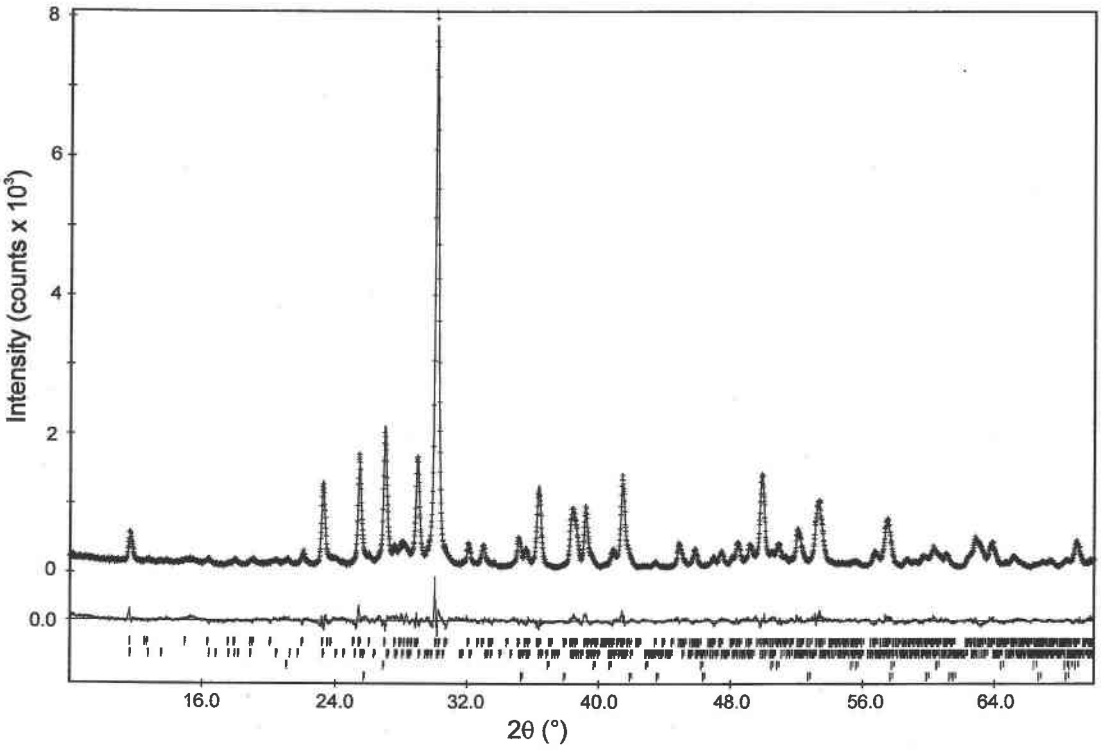

FIG. 2. Rietveld refinement plot for Bril wollastonite concentrate (+: observed intensity at each step, solid line: calculated pattern, solid line below: difference between observed and calculated intensities, vertical bars: positions of all Bragg reflections for (top to bottom) wollastonite-1*A*, wollastonite-2*M*, quartz, corundum).

overlap almost exactly, and it is not possible to resolve them with adequate precision. To overcome this problem, the relative amounts of the polytypes were refined "manually" by adjusting the scale factor of wollastonite-2*M* in the control file and refining only the scale factor of wollastonite-1*A* until a satisfactory fit of the calculated patterns to the observed pattern for both 1*A* and 2*M* polytypes was obtained. As the $21\bar{1}$ reflection of wollastonite-2*M* is the only peak independent of wollastonite-1*A* peaks, it was used in this way to calibrate the amount of wollastonite-2*M* present. The ratio of wollastonite-1*A* to wollastonite-2*M* obtained was 6.4:1 by weight (scale-factor ratio of 25:1). Subsequent refinement of the two wollastonite polytypes in all samples was done by assigning the same position in the refinement matrix to both scale-factors, and by constraining the calculated shifts during least-squares refinement to an amount proportional to the mass fractions of the 1*A* and 2*M* polytypes previously obtained from manually adjusting the scale-factors. Finally, the fit between the calculated and observed patterns was improved sigificantly by refining the atomic position parameters of wollastonite-1*A*. The refined positional parameters are in good agreement with the published values. This method gave superior agreement between the refined and nominal amounts of the total wollastonite present (Fig. 3B).

Details of data collection and Rietveld refinement of the simulated ores are summarized in Table 2; the Rietveld refinement results are summarized in Table 5. A comparison of the nominal abundance of each phase *versus* the experimentally determined abundance is given graphically in Figures 3B–F. In all cases, the agreement between the nominal and experimental values is excellent, and the numerical criteria of goodness of fit, R_p, R_{wp}, R_{exp} and S, uniformly show that the fit of the calculated X-ray patterns to the observed patterns is good. A typical Rietveld refinement plot showing visually the quality of the fits is given in Figure 4 (sample 6, Tables 2, 5).

As the amount of total wollastonite present is vital to the evaluation and processing of such ores, the validity of the Rietveld method in determining its abundance was our major concern in this study. As the estimated standard deviations calculated from Rietveld refinement are unrealistically small (less than 0.1% relative), we

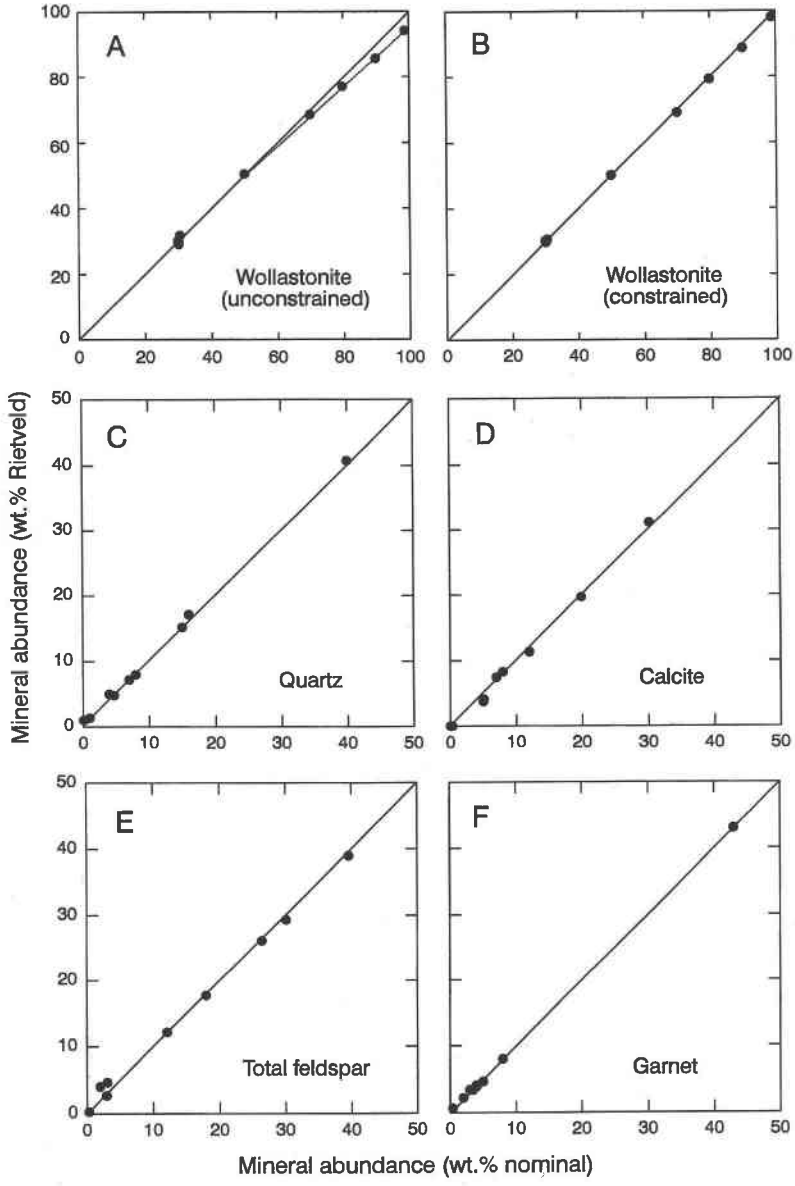

FIG. 3. Plot of nominal abundance of minerals in simulated wollastonite ores determined by weighing *versus* total abundance determined by the Rietveld method. Solid lines represent a 1:1 relationship. A. Wollastonite-1*A* and wollastonite-2*M* refined without constraint. B. Wollastonite-1*A* and wollastonite-2*M* constrained to a ratio of 6.4:1 (wt.%) during refinement. C. Quartz. D. Calcite. E. Total feldspar. F. garnet.

used the "relative error" calculated from the deviation of the Rietveld results from the nominal weights to evaluate the precision of the refinements. Over the range of 30–99 wt.% wollastonite, the agreement between nominal and experimental abundance is excellent (Fig. 3B). The difference between the nominal and experimentally derived amounts ranges from 0.04 to 1.3 wt.% relative (Table 5) and varies randomly. For phases other than the wollastonite, the agreement between nominal and experimental weights generally depends on the amount present. Figure 5 shows the dependence of the relative error in the experimentally de-

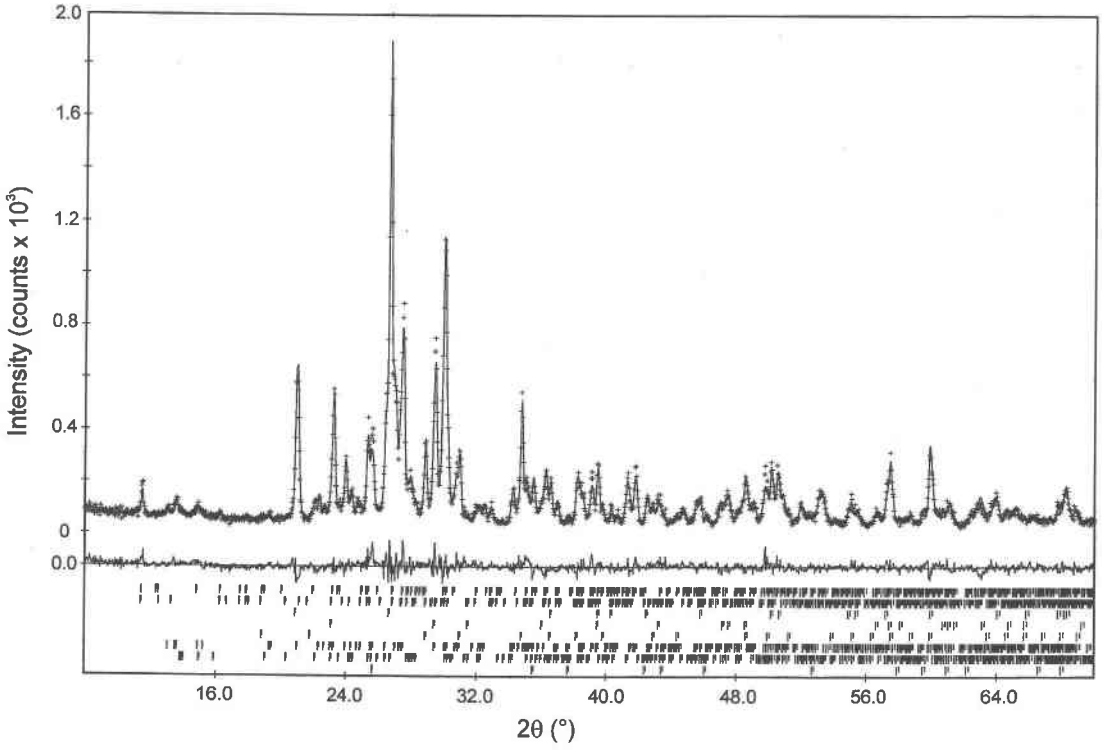

FIG. 4. Rietveld refinement plot for simulated wollastonite ore (No. 6, Tables 2, 5) (+: observed intensity at each step, solid line: calculated pattern, solid line below: difference between observed and calculated intensities, vertical bars: positions of all Bragg reflections for (top to bottom) wollastonite-1*A*, wollastonite-2*M*, quartz, calcite, almandine, microcline, albite, corundum).

rived weights of quartz, calcite, almandine and total feldspar on their concentration. For concentrations above 6 wt.%, the difference between nominal and experimental weights is less than 6% relative, and decreases at high concentrations to about 1%. For concentrations below 6 wt.%, the relative error rises rapidly.

The collection time for each set of step-scan data for the simulated ore samples was 52 minutes (Table 2). In order to determine whether it was possible to get good results in less time, the step interval was doubled to 0.08°2θ at a counting time of 2 s/step for sample 1 (1B, Tables 2, 5); the time for data collection was then 26 minutes. With the exception of almandine, the relative errors for each of the minerals are close to those obtained using a step interval of 0.04°2θ, showing that satisfactory modal analyses of phases present in amounts greater than about 5 wt.% may be obtained in relatively short periods of time. Attempts to decrease collection times by reducing the counting time per step to less than 2 s did not give satisfactory results. Similarly, good results from using relatively short times for data collection (large step-intervals) were obtained by Farkas (1997) and by Raudsepp & Farkas (1997) for the modal analysis of granitic rocks with the Rietveld method and the same experimental conditions as for this study.

Bril drill-core samples

The details of data collection and Rietveld refinement of the drill-core samples from the Bril skarn are summarized in Table 3; the Rietveld refinement results are summarized in Table 6. As for refinements of the simulated samples of ore, the numerical criteria of fit, R_p, R_{wp}, R_{exp} and S show that the fit of the calculated X-ray patterns to the observed patterns is very good. A typical Rietveld refinement plot showing visually the quality of the fits is given in Figure 6 (sample 4820, Tables 3, 6).

Mineral abundances in Bril drill-core samples measured with a Rietveld refinement are compared to those determined by projection in Figures 7A–F. Mineral abundance is plotted as a single point for those phases for which abundance can be uniquely determined by

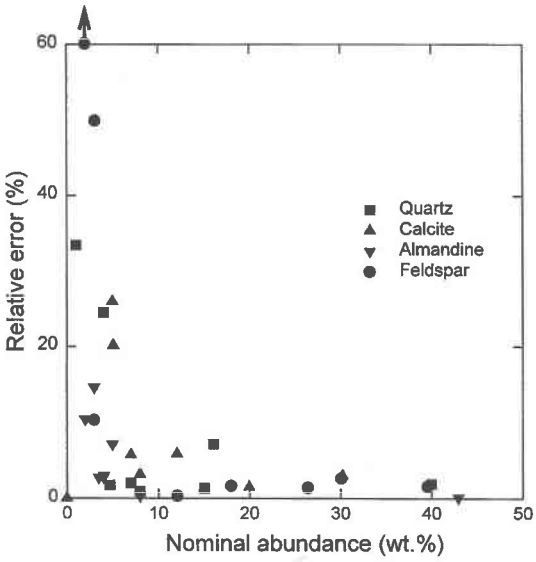

FIG. 5. Plot of nominal abundance of minerals in simulated wollastonite ores determined by weighing *versus* relative error. Relative error = [(|nominal abundance – abundance determined by Rietveld refinement|)] × 100. Point for Sample 4, feldspar (arrow), is plotted off the scale (abundance, 4.03 wt.%; relative error, 98%).

projection methods (Figs. 7E, F). For minerals for which no unique solution is possible, the range of abundance is indicated by horizontal lines (Figs. 7A–D). The mismatch between mineral abundance as determined by the Rietveld method *versus* the projection method is significant and indicated by the extent to which data fall off the lines of slope = 1.0 in Figure 7. The mismatch may derive from errors in either method, but given that the Rietveld method was accurate in determining mineral abundance in synthetic skarn samples, we looked first to errors or invalid assumptions in the projection method to explain the discrepancy. For phases with abundance greater than about 5 mole %, the mismatch between the projection and Rietveld methods can be attributed to shortcomings in the basis-transformation or methods of whole-rock chemical analysis upon which the projection is dependent.

Determinations of wollastonite abundance by the two methods are in excellent agreement for samples with wollastonite contents in excess of 40 mole % (Fig. 7a). The two methods are also in excellent agreement for samples with very small amounts of wollastonite (<2 mole %) (4 samples; Fig. 7A, Table 6). For those samples with a significant range in permitted wollastonite content as determined by projection, measurements by the Rietveld method generally lie at or near the maximum of that range. For several samples with intermediate contents of wollastonite, the projection method consistently estimates lower contents of wollastonite than the Rietveld method. These samples (6360, 5000 and 4400) contain mineral assemblages atypical for the Isk wollastonite skarns (Table 6, Jaworski & Dipple 1996). The discrepancy between the two methods therefore most likely results from invalid assumptions in the projection. For example, samples 5000 and 4400 both contain a substantial proportion of plagioclase, which the basis-transformation does not accommodate. The remaining sample (6360) contains an unusually large amount of calcite, and the discrepancy in wollastonite content is complemented by a mismatch in calcite content. This sample is discussed in more detail below.

The abundance of garnet, pyroxene and quartz, as determined by the projection method, spans a significant range (Figs. 7B–D). Mineral abundance as determined by Rietveld analysis generally falls at or near the minimum level of garnet and quartz abundance and at or near the maximum in pyroxene abundance. The reaction relationship involving these minerals dictates that as garnet and quartz content is minimized, the content of pyroxene and wollastonite is maximized. It is therefore encouraging that the Rietveld estimates of wollastonite abundance also fall at or near the maximum of the range estimated from whole-rock composition. These relationships are consistent with the field observations that diopside is much more abundant than garnet in the skarn, and that skarn zones are dissected by a series of pyroxenite dikes from the Zippa syenite pluton (Lueck & Russell 1995, Jaworski & Dipple 1996).

The abundances of titanite and apatite as measured by the two methods are generally consistent, but exhibit considerable scatter (Fig. 7E). We consider apatite abundance measured by the projection method reliable because it derives directly from the whole-rock phosphorus content as measured by X-ray-fluorescence spectroscopy. The discrepancy between apatite abundance measured by Rietveld and that measured by projection can be attributed to the imprecision of Rietveld methods for low-abundance minerals (*cf.* Figs. 5, 7E). The Rietveld determination of titanite abundance also is imprecise because of the low abundance of this mineral in the Isk skarn samples (Fig. 7E). However, titanite abundance as measured by the projection method is equally suspect because the basis-transformation does not allow for the observed substitution of titanium into garnet (Gordon & Dipple 1999). Neither method can be relied upon to provide a precise determination of titanite content.

Calcite and feldspar abundance as measured by the two methods is in good agreement, although there is a systematic deviation between the projection and Rietveld estimates that can be attributed to invalid assumptions adopted in the projection method. The basis-transformation assigns all K and Na to alkali feldspar. However, pyroxene within the Isk deposits contains up to 2 wt.% Na_2O (Raudsepp, unpubl. electron-probe data). Attributing all Na to feldspar therefore leads to

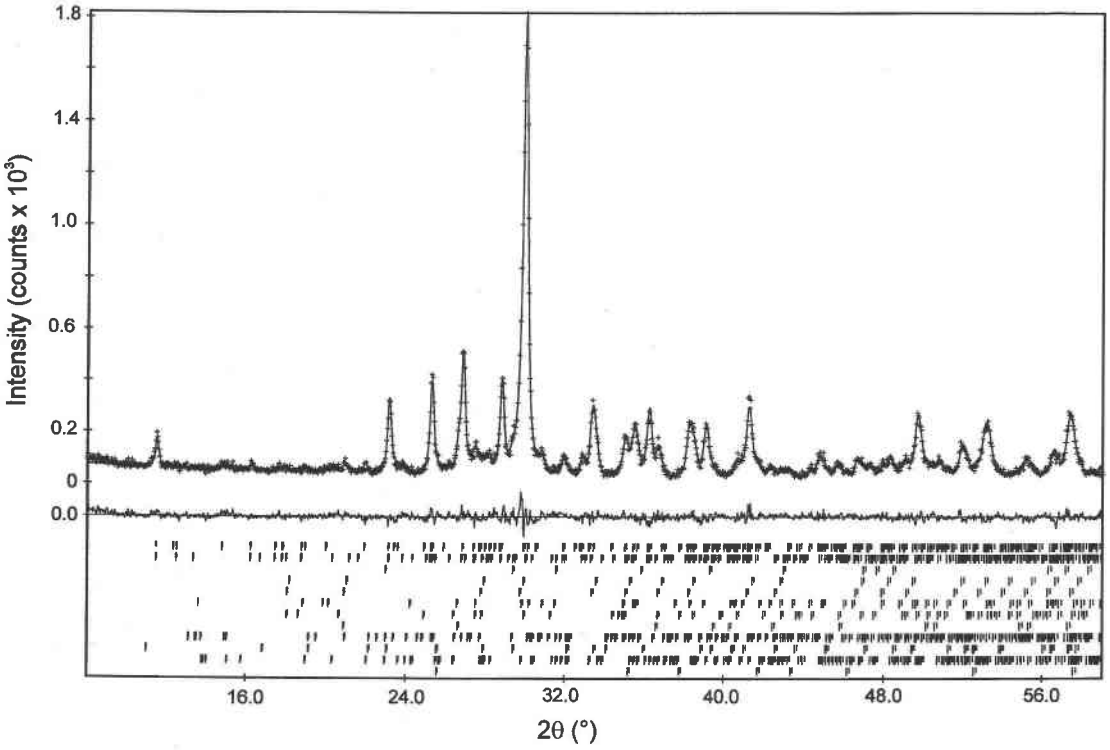

FIG. 6. Rietveld refinement plot for wollastonite ore (No. 4820, Table 3, 6) (+: observed intensity at each step, solid line: calculated pattern, solid line below: difference between observed and calculated intensities, vertical bars: positions of all Bragg reflections for (top to bottom) wollastonite-1*A*, wollastonite-2*M*, calcite, grossular, andradite, pyroxene, titanite, quartz, microcline, apatite, plagioclase, corundum).

an overestimate of feldspar content in Bril samples. The abundance of calcite determined by projection also is systematically higher than measurements by the Rietveld method. We assign this mismatch to the projection method because it must rely on L.O.I. for calcite content. The error is largest in sample 6360, which contains an unusually large amount of calcite and has a L.O.I. of 15.74%. A more accurate determination of calcite content by projection requires direct determination of the CO_2 content. This error is also reflected in a mismatch in wollastonite abundance for this sample.

For phases with abundance greater than about 5 mole %, the discrepancies between mineral abundance as estimated by Rietveld and projection methods can be attributed to problems with the projection method. However, the errors that we have identified cannot be accommodated with our basis-transformation formulation and whole-rock analytical methods. In the companion paper, a new whole-rock chemical method is described that relies on linear programming to accommodate additional variance in mineral composition (Gordon & Dipple 1999). Despite its shortcomings, the projection method accurately estimates wollastonite content (Fig. 7A) and is being used by our industrial partner to determine the economic potential of wollastonite in the Isk skarns as an industrial mineral deposit.

CONCLUSIONS

We have shown that accurate and precise abundances of wollastonite and associated minerals in skarn may be obtained with the Rietveld method and X-ray powder-diffraction data from large, heterogeneous samples that contain up to 13 phases. We evaluated the potential of the Rietveld method for this purpose by first analyzing a suite of simulated wollastonite ores with known mineral compositions and modes. The X-ray-diffraction data were collected under conditions optimized for measurement of wollastonite abundance in the range of about 20–100 wt.%; in this regard, we were able to measure wollastonite content with relative error better than 1.3%. The abundance of associated minerals was determined with a precision that depended on their concentration. Typically, relative errors of less

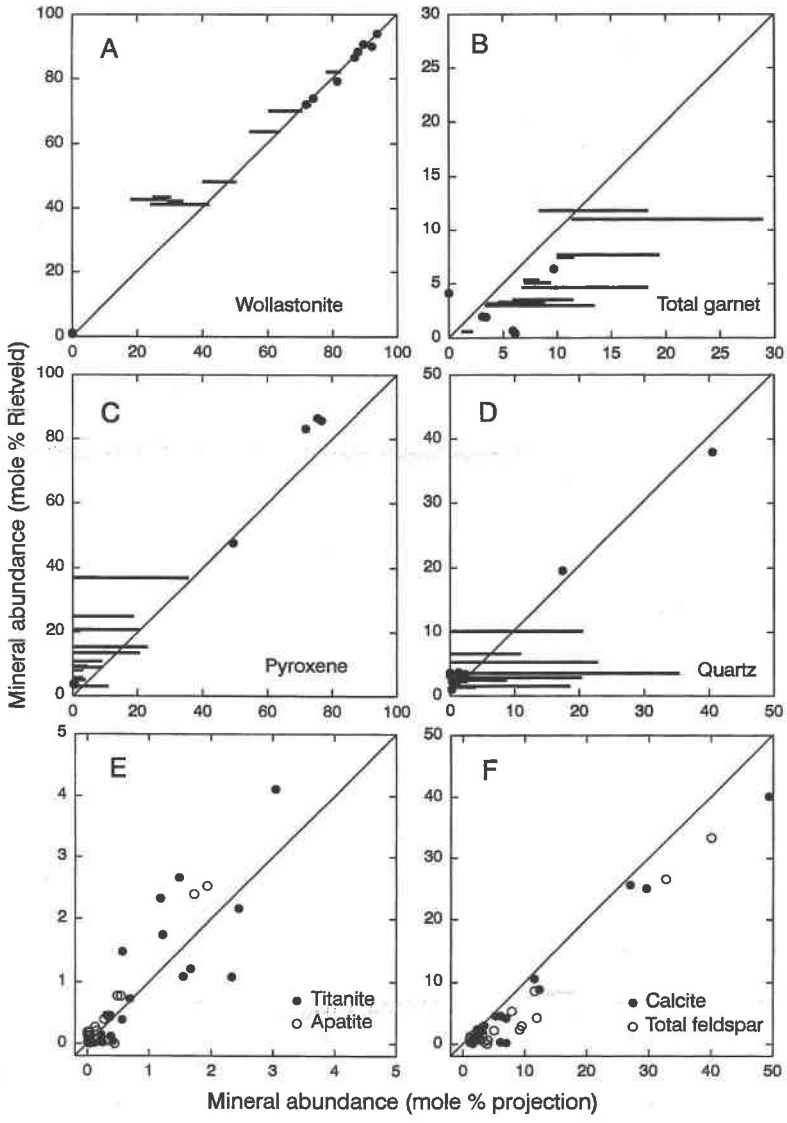

FIG. 7. Plot of nominal abundance of minerals in Bril drill-core samples determined by the projection method *versus* total abundance determined by the Rietveld method. Single points indicate that abundance was uniquely determined by the projection method; horizontal bars indicate that no unique solution was possible; they show the range. Solid lines represent a 1:1 relationship. A. Total wollastonite. B. Garnet. C. Calcic pyroxene. D. Quartz. E. Titanite and apatite. F. Total feldspar and calcite.

than 6% were obtained for concentrations greater than about 6 wt.%; below this concentration, relative errors increased to 100%. Furthermore, accurate and precise results for the major phases present were obtained using relatively short times for the acquisition of the X-ray data; data-acquisition time for the simulated and natural ores was 52 and 43 minutes, respectively, but data with not significantly inferior precision can be acquired in 26 minutes by doubling the step interval.

An evaluation of the accuracy and precision was more difficult for the natural ores than for the simulated samples, as the abundances of reference minerals determined by the projection method were not accurate for all of the unusually large range of rock compositions

analyzed. Wollastonite abundances measured with the Rietveld method were found to be either in excellent agreement with those determined by the projection method (>40 mole %, <2 mole %), or at or near the maximum range of the calculated amounts. Agreement between the two methods for the other minerals was not as consistent as for the wollastonite, but generally Rietveld-derived mineral abundances were near the minimum or maximum estimates of those determined by the projection method. For phases with an abundance greater than about 5 mole %, we attribute these discrepancies between mineral abundance as estimated by the Rietveld and projection methods to problems with the whole-rock analytical methods or basis-transformation used by the projection method. However, methods of estimation based on whole-rock composition data provide more accurate determination of mineral abundance than Rietveld methods for minor phases that accumulate incompatible elements. We are confident that our estimates of mineral abundances in skarn from Rietveld refinement of the natural ores are not significantly different with regard to accuracy and precision from those obtained for the simulated reference samples.

Acknowledgements

Financial support for this work was provided by Natural Sciences and Engineering Research Council of Canada (research grant to MR and grant IOR195826 to GMD) and Whitegold Resources Inc. of Vancouver, B.C. We thank Annette Bingemer for assistance in the preparation of synthetic skarn samples, and Bart Jaworski, Brian Lueck and Allen Achilles of Whitegold Resources for their support. The paper was significantly improved by helpful suggestions from reviewers Ian Madsen and Jeffrey Post, and by the editorial comments of Robert Martin.

References

Armbruster, T., Bürgi, H.B., Kunz, M., Gnos, E., Brönnimann, S. & Lienert, C. (1990): Variation of displacement parameters in structure refinements of low albite. *Am. Mineral.* **75**, 135- 140.

_____, Geiger, C.A. & Lager, G.A. (1992): Single-crystal X-ray structure study of synthetic pyrope almandine garnets at 100 and 293 K. *Am. Mineral.* **77**, 512-521.

Baerlocher, C. & Schicker, P. (1987): X-ray Rietveld structure refinement of monoclinic ZSM-5. *Acta Crystallogr.* **A43**, *Suppl.*, C-233.

Bish, D.L. (1993): Rietveld refinement of the kaolinite structure at 1.5 K. *Clays Clay Minerals* **41**, 738-744.

_____ & Howard, S.A. (1988): Quantitative phase analysis using the Rietveld method. *J. Appl. Crystallogr.* **21**, 86-91.

_____ & Post, J.E. (1993): Quantitative mineralogical analysis using the Rietveld full-pattern fitting method. *Am. Mineral.* **78**, 932-940.

Brigatti, M.F. & Davoli, P. (1990): Crystal-structure refinements of 1*M* plutonic biotites. *Am. Mineral.* **75**, 305-313.

Brindley, G.W. (1945): The effect of grain or particle size on X-ray reflections from mixed powders and alloys, considered in relation to the quantitative determination of crystalline substances by X-ray methods. *Phil. Mag.* **36**, *Ser.* **7**, 347-369.

Caglioti, G., Paoletti, A. & Ricci, F.P. (1958): Choice of collimators for a crystal spectrometer for neutron diffraction. *Nucl. Instrum.* **3**, 223-228.

Dal Negro, A., De Pieri, R., Quareni, S. & Taylor, W.H. (1978): The crystal structures of nine K feldspars from the Adamello Massif (northern Italy). *Acta Crystallogr.* **B34**, 2699-2707.

Effenberger, H., Mereiter, K. & Zemann, J. (1981): Crystal structure refinements of magnesite, calcite, rhodochrosite, siderite, smithsonite, and dolomite, with discussions of some aspects of the stereochemistry of calcite-type carbonates. *Z. Kristallogr.* **156**, 233-243.

Farkas, P.W. (1997): *Rapid Quantitative Phase Analysis of Rocks by Rietveld Structure Refinement of X-Ray Powder-Diffraction Data*. B.Sc. thesis, Univ. of British Columbia, Vancouver, British Columbia.

Gordon, T.M. & Dipple, G.M. (1999): Measuring mineral abundance in skarn. II. A new linear programming formulation and comparison with projection and Rietveld methods. *Can. Mineral.* **36**, 17-26.

Hawthorne, F.C., Groat, L. A., Raudsepp M., Ball, N. A, Kimata, M., Spike, F.D., Gaba, R., Halden, N.M, Lumpkin, G.R., Ewing R. C., Greegor, R.B., Lytle, F.W., Ercit, T.S., Rossman, G.R., Wicks, F. J, Ramik, R.A., Sherriff, B.L., Fleet, M.E. & McCammon, C. (1991): Alpha-decay damage in titanite. *Am. Mineral.* **76**, 370-396.

Hazen, R.M. & Finger, L.W. (1978): Crystal structures and compressibilities of pyrope and grossular to 60 kbar. *Am. Mineral.* **63**, 297-303.

Heller, L. & Taylor, H.F.W. (1956): *Crystallographic Data for the Calcium Silicates*. H.M.S.O., London, U.K.

Hill, R.J. (1984): X-ray powder diffraction profile refinement of synthetic hercynite. *Am. Mineral.* **69**, 937-942.

_____ (1991): Expanded use of the Rietveld method in studies of phase abundance in multiphase mixtures. *Powd. Diff.* **6**, 74-77.

_____ & Howard, C.J. (1987): Quantitative phase analysis from neutron powder diffraction data using the Rietveld method. *J. Appl. Crystallogr.* **20**, 467-474.

_____, TSAMBOURAKIS, G. & MADSEN, I.C. (1993): Improved petrological modal analyses from X-ray powder diffraction data by use of the Rietveld method. I. Selected igneous, volcanic, and metamorphic rocks. *J. Petrol.* **34**, 867-900.

HUGHES, J.M., CAMERON M. & CROWLEY, K.D. (1989): Structural variations in natural F, OH, and Cl apatites. *Am. Mineral.* **74**, 870-876.

JAWORSKI, B. & DIPPLE, G.M. (1996): Zippa Mountain wollastonite skarns, Iskut River map area. *In* Geological Fieldwork 1995. *British Columbia Ministry of Energy, Mines and Petroleum Resources, Pap.* **1996-1**, 243-249.

LAGER, G.A., ARMBRUSTER, T., ROTELLA, F.J. & ROSSMAN, G.R. (1989): OH substitution in garnets: X-ray and neutron diffraction, infrared and geometric-modeling studies. *Am. Mineral.* **74**, 840-851.

LE PAGE, Y. & DONNAY, G. (1976): Refinement of the crystal structure of low-quartz. *Acta Crystallogr.* **B32**, 2456-2459.

LEVIEN, L. & PREWITT, C.T. (1981): High-pressure structural study of diopside. *Am. Mineral.* **66**, 315-323.

LEWIS, J., SCHWARZENBACH, D. & FLACK, H.D. (1982): Electric field gradients and charge density in corundum, α-Al_2O_3. *Acta Crystallogr.* **A38**, 733-739.

LUECK, B.A. & RUSSELL, J.K. (1995): Geology and origins of the Zippa Mountain igneous complex with emphasis on the Zippa Mountain pluton, northern British Columbia. *Geol. Surv. Can., Current Research* **1994-A**, 77-85.

MAKINO, K. & TOMITA, K. (1989): Cation distribution in the octahedral sites of hornblendes. *Am. Mineral.* **74**, 1097-1105.

MUMME, W.G., TSAMBOURAKIS, G. & CRANSWICK, L. (1996b): Improved petrological modal analyses from X-ray and neutron powder diffraction data by use of the Rietveld method. III. Selected massive sulfide ores. *Neues Jahrb. Mineral., Abh.* **170**, 231-255.

_____, _____, MADSEN, I.C. & HILL, R.J. (1996a): Improved petrological modal analyses from X-ray powder diffraction data by use of the Rietveld method. II. Selected sedimentary rocks. *J. Sed. Res.* **66**, 132-138.

OHASHI, Y. (1984): Polysynthetically-twinned structures of enstatite and wollastonite. *Phys. Chem. Minerals* **10**, 217-229.

PHILLIPS, M.W., COLVILLE, A.A. & RIBBE, P.H. (1971): The crystal structures of two oligoclases: a comparison with low and high albite. *Z. Kristallogr.* **133**, 43-65.

POST, J.E. & BISH, D.L. (1989): Rietveld refinement of crystal structures using powder X-ray diffraction data. *Rev. Mineral.* **20**, 277-308.

RAUDSEPP, M. & FARKAS, P.W. (1997): Rapid quantitative mineralogical analysis of rocks by Rietveld structure refinement using X-ray powder diffraction data. *Geol. Assoc. Can. – Mineral. Assoc. Can., Program Abstr* **22**, A124.

_____, HAWTHORNE, F.C. & TURNOCK, A.C. (1990): Evaluation of the Rietveld method for the characterization of fine-grained products of mineral synthesis: the diopside–hedenbergite join. *Can. Mineral.* **28**, 93-109.

RIETVELD, H.M. (1967): Line profiles of neutron powder-diffraction peaks for structure refinement. *Acta Crystallogr.* **22**, 151-152.

_____ (1969): A profile refinement method for nuclear and magnetic structures. *J. Appl. Crystallogr.* **2**, 65-71.

THOMPSON, J.B., JR. (1982): Composition space: an algebraic and geometric approach. *Rev. Mineral.* **10**, 1-31.

YOUNG, R.A. (1995): DBWS-9411 – an upgrade of the DBWS programs for Rietveld, refinement with PC and mainframe computers. *J. Appl. Crystallogr.* **28**, 366-367.

_____, MACKIE, P.E. & VON DREELE, R.B. (1977): Application of the pattern-fitting structure-refinement method to X-ray powder diffractometer patterns. *J. Appl. Crystallogr.* **10**, 262-269.

_____, SAKTHIVEL, A., MOSS, T.S. & PAIVA-SANTOS, C.O. (1994): *User's guide to program DBWS-9411 for Rietveld, analysis of X-ray and neutron powder diffraction patterns.* School of Physics, Georgia Institute of Technology, Atlanta, Georgia.

Received April 16, 1998, revised manuscript accepted July 28, 1998.